TECHNICAL PAPER

ISSN 1047-3289 *J. Air & Waste Manage. Assoc.* **51**:121-132

Observations and Model Simulations of Carbon Monoxide Emission Factors from a California Highway

Anthony E. Held, Daniel P.Y. Chang, and Debbie A. Niemeier

Department of Civil and Environmental Engineering, University of California, Davis

ABSTRACT

A series of twelve intensively monitored 1-hr CO dispersion studies were conducted near Davis, CA, in winter 1996. The experimental equipment included twelve CO sampling ports at elevations up to 50 m, three sonic anemometers, a tethersonde station, aircraft measurements of wind and temperature profile aloft, and a variety of conventional meteorological equipment. The study was designed to explore the role of vehicular exhaust buoyancy during worst-case meteorological conditions, such as low winds oriented in near-parallel alignment with the road during a surface-based nocturnal inversion. From the study, field estimates of the CO emission factor (EF) from a California vehicle fleet were computed using two different methods. The analysis suggests that the CT-EMFAC/EMFAC (EMission FACtor) models currently used to conduct federal conformity modeling significantly overpredict CO emissions for high-speed, free-flowing traffic on California highways.

INTRODUCTION

Transportation projects using federal funding are required to undergo a review of their environmental impacts during the planning and design process as specified in conformity regulations. Regional and localized air quality studies are often part of the impact assessment procedure.[1] Microscale modeling of air pollutants near roadways in California is typically accomplished using two models, one to estimate fleet averaged emissions factor (EF), such as the California Department of Transportation's (CALTRANS) CT-EMFAC (EMission FACtor) model, and one to model dispersion of pollutants, such as the CALINE4 model.

IMPLICATIONS

The California Department of Transportation (CALTRANS) currently uses EMFAC to predict regional emission factors. For lack of a more appropriate model, transportation planners routinely use CT-EMFAC, a streamlined version of EMFAC, to conduct microscale modeling for federal conformity requirements. This study indicates that CT-EMFAC/EMFAC models may significantly overpredict CO emission factors for free-flowing, high-speed interstate highways. These results further emphasize the need for appropriate emission models to increase the reliability of microscale analyses.

In October 1995, the University of California, Davis (UCD), in conjunction with the UCD-CALTRANS Air Quality Project, began an investigation to determine if the CALINE family of models adequately parameterized the effect of vehicular exhaust buoyancy during "worst-case" meteorological events. The intensive sampling effort, conducted near California Interstate 80 (I-80), included a variety of sampling towers, meteorological balloons, and aircraft sampling. In addition to specifying near-roadway meteorological fields, the collected data proved ideal for calculating field-estimated CO EFs. This paper details how site-specific CO EFs can be determined based on integrating near-roadway wind and pollutant profiles. A novel approach to "back-calculate" a CO EF based on the CALINE4 dispersion model is also developed. Lastly, a comparison between the regulatory model CT-EMFAC and experimentally determined CO EFs is presented.

To better understand why this analysis is insightful, it is useful to understand the history and development of the EMFAC and CT-EMFAC models. EMFAC is designed for use with area inventory models such as BURDEN. These area inventory models use input from EMFAC and standard travel demand models, which produce outputs of vehicle miles traveled (VMT), to estimate mobile-source pollutant inventories for urban airsheds. The EMFAC emission rates are based on cycles that represent average trips and use average speed as an identifier for trip-based mobile-source emissions.[2] Obviously, it is desirable to have fleet-averaged, aggregate EFs based on speed that is trip-averaged, rather than instantaneous, to estimate airshed pollutant loads.

CT-EMFAC was developed as a "front-end" to EMFAC[3,4] and became the de facto model used for microscale modeling in California. However, given that the EMFAC model was not designed for microscale modeling,

its performance is suspect when using it for this purpose. One of the most significant drawbacks of using EMFAC for microscale modeling is that the microscale modeler is trying to estimate a *modal* emission factor based on a trip-averaged, or *aggregate*, EF model. For instance, in this paper we determined the CO EF from a California fleet that is traveling 65–70+ mph (i.e., a modal EF).

A recent study by the National Research Council noted the need for a toolbox of modeling tools based on the analysis conditions.[5] Our analysis supports this notion and the findings of previous microscale modeling studies.[6-8] We clearly demonstrate that using a trip-averaged EF model to determine localized emissions is inappropriate.

SAMPLING SITE DESCRIPTION

In a multi-month study performed near Davis, CA, eight fixed stations and one aircraft were used to collect pollutant and meteorological data along the I-80 corridor. The fixed stations included two 18-m and one 6-m sampling tower, one sampling balloon, one tethersonde, one low-resolution video camera, two CO autosamplers, and three sonic anemometers. The function and usage of the various sampling stations are presented in Tables 1 and 2. The station locations and their relation to the observed highway are shown in Figure 1. Station labels in this figure correspond with those used in Tables 1 and 2. The meteorological instruments and CO sampling ports on the balloon and tower stations are shown in Figures 2, 3, and 4. Most of the instrumentation was placed south of the roadway because the predominant daily seasonal wind direction is from the north. Measurements were collected on 7 days when meteorological conditions were forecasted to be favorable. Six of the seven experiments were conducted between 6:00 and 8:00 a.m.; the seventh experiment was conducted between 6:00 and 8:00 p.m.

Table 1. Sampling station functions.

Station	Function
A. North 18-m tower (32)[a]	Heat and momentum fluxes; wind, temperature, and CO profiles
B. Call box 1-D sonic (3.6)	Highway heat flux
C. Freeway 6-m tower (14)	Heat and momentum fluxes; CO profiles
D. South 18-m tower (54)	Wind, temperature, and CO profiles
E. Balloon station (117)	High-elevation CO profiles
F. Tethersonde station (177)	High-elevation wind, temperature, and RH profiles
G. Aircraft (variable)	Boundary-layer wind and temperature profiles
H. Camera station	Traffic volume
I. CO auto samplers (variable)	Remote determination of ground-level CO concentrations

[a]Approximate distance in meters to the nearest traveled way of I-80.

Table 2. Experiment dates and configurations.

Sampling Period	Stations Used
Nov 14, 1996, 6:00–8:00 a.m.	A,B,D,E,G,H
Nov 21, 1996, 6:00–8:00 a.m.	A,B,D,E,F,H,I
Nov 26, 1996, 6:00–8:00 a.m.	A,B,C,D,H,I
Dec 1, 1996, 6:00–8:00 p.m.	A,C,D,E,F,G,I
Dec 3, 1996, 6:00–8:00 a.m.	A,B,C,D,E,F,G,H,I
Jan 8, 1997, 6:00–8:00 a.m.	A,B,C,D,E,F,H,I
Jan 10, 1997, 6:00–8:00 a.m.	A,B,C,D,E,F,H,I

Five-minute grab samples were collected at multiple elevations using diaphragm pumps, neoprene tubing, and Tedlar bags at each of the CO sampling stations. Samples were typically collected every 10 min from 6:00 to 8:00 a.m. except during unfavorable meteorological conditions. The Tedlar sampling bags were transported to a UCD lab and analyzed with two Dasibi non-dispersive infrared CO analyzers within 36 hr of sampling in all cases and within 24 hr in most cases.

Meteorological field variables were collected at each of the 18-m tower locations by data loggers at 1 Hz. Each 18-m tower included four temperature sensors housed in both aspirated and non-aspirated radiation shields, two conventional cup anemometer/wind-vane systems, and one UVW propeller system. Campbell CSAT-3 3-D sonic anemometers, which sampled wind speed and temperature at 10 Hz, were mounted on the northern 18-m tower and the southern 6-m tower at an elevation of ~6 m. In addition, a 1-D sonic was attached ~3.6 m from the traveled way to a roadway call box (see Figure 1, Station B) so that the nearside roadway heat flux could be determined.

The tethersonde, balloon, and aircraft measurements complemented ground-based instrumentation and allowed a detailed description of the planetary boundary layer to be ascertained. The tethersonde system was used to continuously profile wind speed, direction, pressure, temperature, and relative humidity up to an elevation of ~45 m. The aircraft collected upper elevation temperature and wind profiles. Finally, eastbound and westbound hourly traffic data were collected using CALTRANS automatic loop detectors located near the experimental site. A low-resolution video camera also continuously recorded the eastbound traffic, which was useful in determining vehicle type and speed estimates, but was not of sufficient resolution to determine vehicle license plate numbers.

Sampling Results

A complete description of the meteorological data and trace gas concentrations collected during the study will not be presented since they are not essential for the subsequent

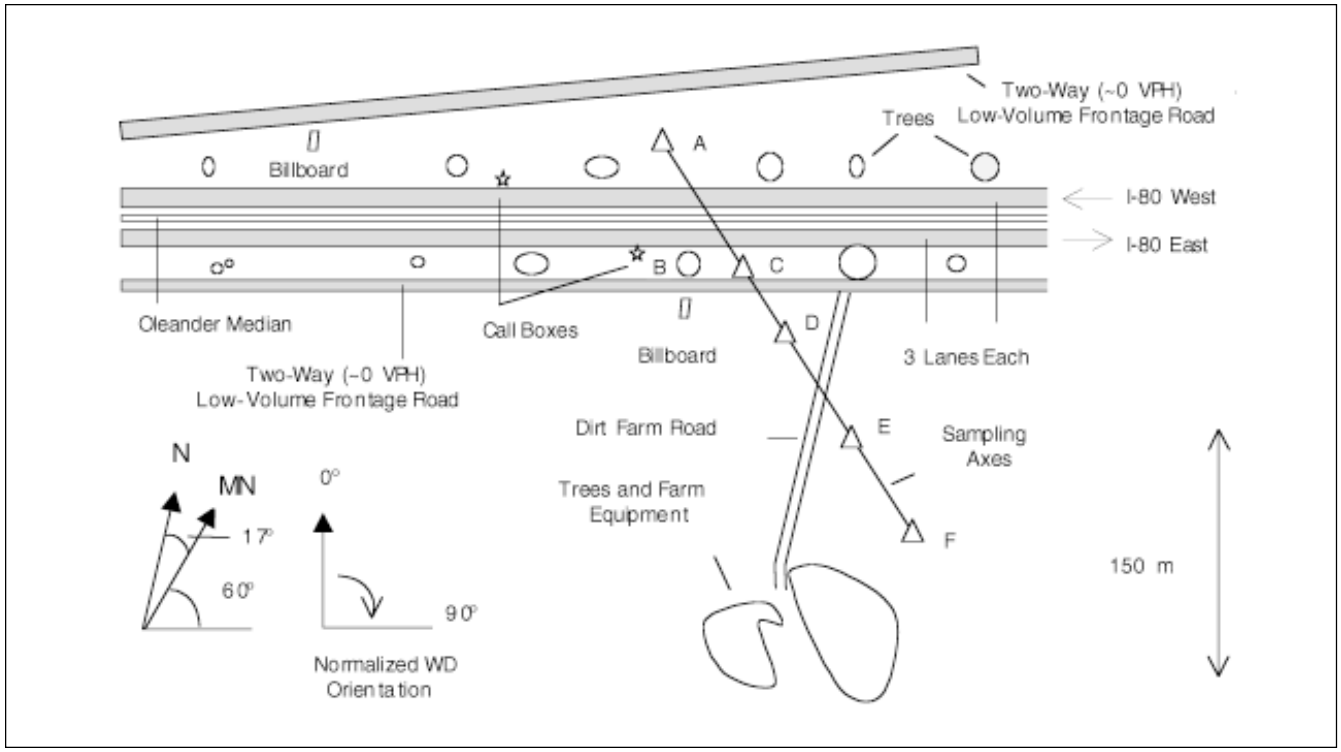

Figure 1. Sampling station locations.

analysis. Interested readers can review Held et al.[9] for additional results and findings. One-hour averaged traffic counts, wind speed, wind direction, vertical heat flux, temperature, and CO concentrations collected at the 18-m towers for the continuous sampling periods are detailed in Table 3. The "background" CO concentration was assumed to be the 18-m CO concentration at the upwind tower (the north tower was typically upwind). The wind

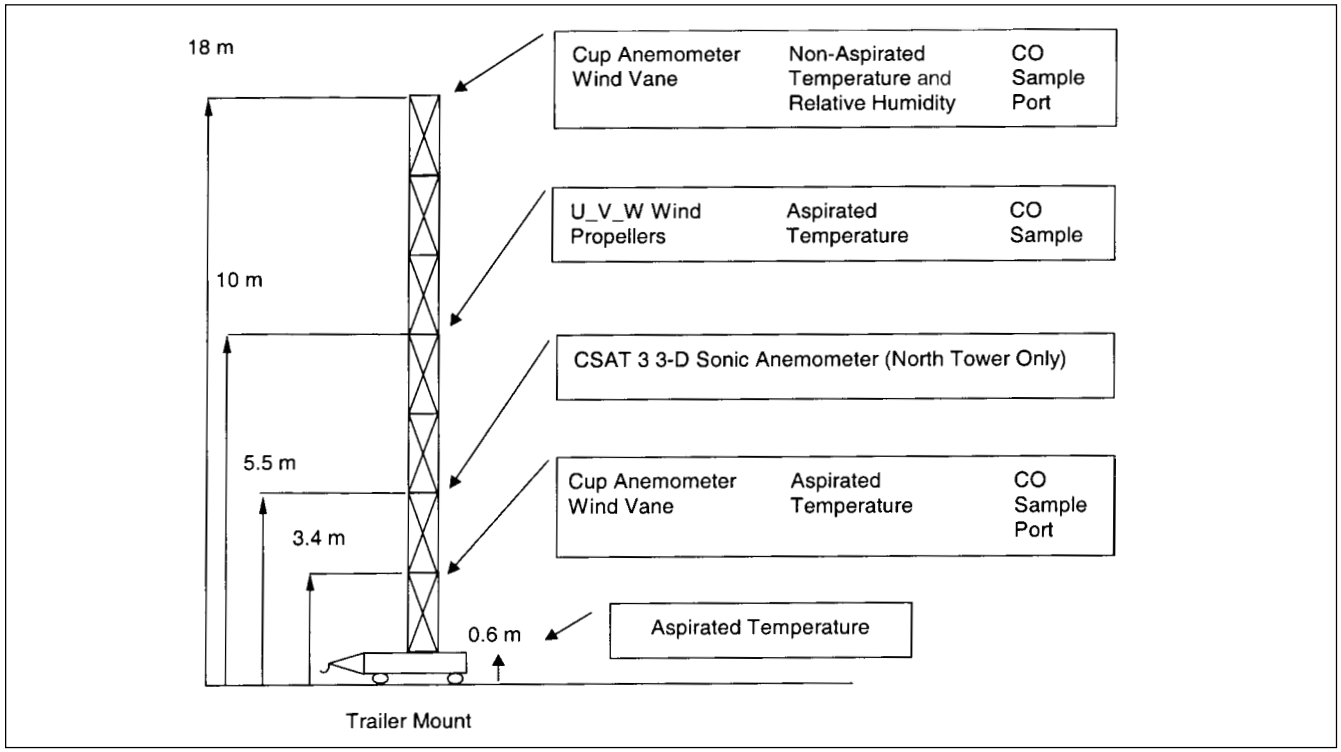

Figure 2. North and south 18-m sampling towers.

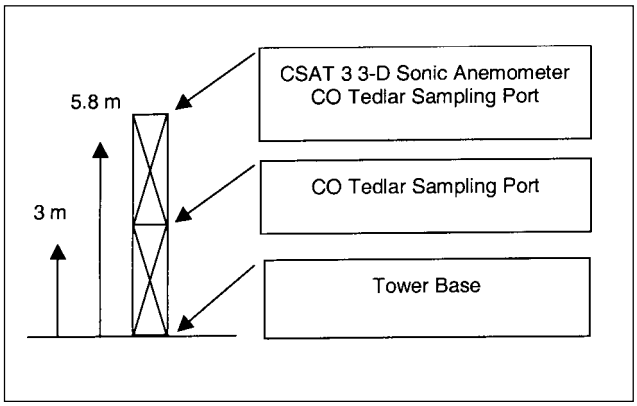

Figure 3. 6-m sampling tower.

directions follow standard meteorological convention (i.e., wind angle is the direction from which the wind is blowing). In addition, wind angles were aligned so that a wind blowing perpendicular to the road from north to south was 0° and a wind parallel to the road from east to west was 90°. The error associated with the standard meteorological equipment for 1-hr averages is variable and instrument-specific. The cup-vane systems used in this project are accurate to ± 3° and within ±0.2 m/sec. Sonic anemometer wind speed and direction error is essentially negligible for our purposes, but the interpretation of the heat fluxes is quite complex (readers are referred to Wilson and Swaters[10] for additional details).

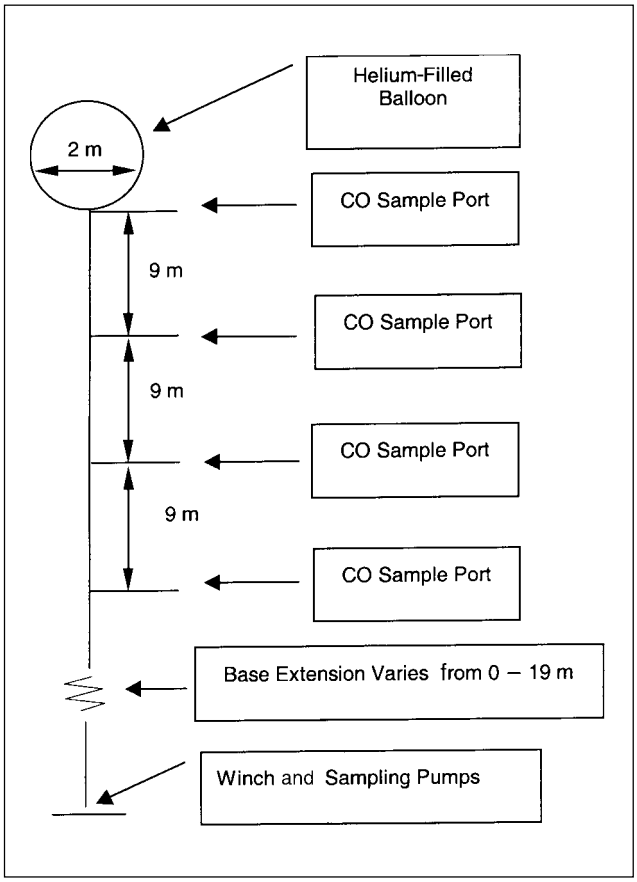

Figure 4. CO sampling balloon.

Trace Gas Error Analysis

Given the high signal-to-noise ratio present in the 5-min averaged CO concentrations, an error analysis is essential to determine the validity of the EF analysis presented in this paper. Furthermore, since many sampling efforts hinge on the averaging of representative "grab-samples", it is instructive to demonstrate that our method of error analysis can be extended to similarly conducted trace gas sampling efforts. The 5-min averaged CO concentrations measured in this study were typically less than 2 parts per million by volume (ppmv), and the Dasibi CO analyzer used for this project was accurate to ±0.1 ppmv. To determine the signal-to-noise ratio for the 1-hr calculations, the functional form of the 1-hr average was assumed to be

$$CO_{1HR} = \sum_{i=1}^{N} \frac{CO_i}{N} \quad (1)$$

where CO_{1HR} is 1-hr average CO concentration (ppmv); CO_i is 5-min averaged CO concentration (ppmv); and N is number of 5-min periods considered in an hourly average (typically 6). The error in the 1-hr average CO measurement can be computed as

$$\sigma_{AVG} = \sqrt{\sum_{i=1}^{N} \left(\frac{\partial CO_{1Hr}}{\partial CO_i} \right)^2 \sigma_i^2} \quad (2)$$

where σ_{AVG} is the standard deviation of the 1-hr averaged CO concentration (ppmv), and σ_i is the standard deviation of the 5-min averaged CO concentration (ppmv). Since the σ_i are all assumed to be identical, eq 2 reduces to

$$\sigma_{1HR} = \sigma_i \sqrt{\frac{1}{N}} \quad (3)$$

Equations 1–3 require that a sequential measure of CO over a time period is identical for several simultaneous samples. This is not an arbitrary assumption made to facilitate the error analysis. Rather, it is a direct consequence of assuming that the wind and pollutant covariance structure near a roadway are statistically stationary for certain averaging periods (in this case, 1 hr). Although most natural processes are far from statistically stationary, the assumption is always explicitly, or implicity, made in the development of steady-state models such as a Gaussian dispersion model. Thus, calculations made with eqs 1–3 are suitable for comparison with any steady-state model or any other measurement that assumes statistical stationarity.

From the equations above, it can be shown the standard deviation of a 1-hr average CO concentration will be 0.041 ppmv based on a 5-min standard deviation of 0.1 ppmv.

Table 3. One-hour averaged meteorological and pollutant concentrations at the north and south 18-m tower stations with traffic counts.

	Nov 14 6:00–7:00 a.m.		Nov 14 7:00–8:00 a.m.		Nov 21 6:00–7:00 a.m.		Nov 21 7:00–8:00 a.m.		Nov 26 6:00–7:00 a.m.		Nov 26 7:00–8:00 a.m.		Dec 1 6:00–7:00 p.m.		Dec 1 7:00–8:00 p.m.		Dec 3 6:00–7:00[a] a.m.		Jan 8 6:00–7:00[a] a.m.		Jan 10 6:00–7:00 a.m.		Jan 10 7:00–8:00 a.m.	
	S	N	S	N	S	N	S	N	S	N	S	N	S	N	S	N	S	N	S	N	S	N	S	N
4.1-m WS[b]	2.1	2.0	1.9	2.0	1.4	1.2	1.3	1.1	4.7	5.6	4.7	NA	1.6	1.4	1.7	1.6	2.1	2.2	1.8	2.0	2.0	2.1	1.7	1.7
5.8-m WS[c]	2.4	2.0	2.5	1.8	NA	1.3	NA	1.1	5.3	6.1	NA	NA	1.6	1.6	1.7	1.7	2.2	2.2	2.1	2.1	NA	NA	NA	NA
11.1-m WS	2.7	2.9	2.6	2.7	1.4	1.4	1.3	1.2	5.8	6.3	5.4	NA	NA	2.1	NA	2.1	2.6	2.6	NA	2.4	NA	2.3	NA	1.8
18.9-m WS	3.6	3.9	3.8	4.1	2.2	2.1	2.0	1.9	8.7	9.1	8.0	NA	3.0	3.1	3.6	3.6	4.3	4.2	3.5	3.6	2.8	2.8	2.2	2.3
4.1-m WD[d]	293	NA	301	NA	320	323	337	347	337	338	334	NA	321	307	318	305	155	142	150	137	322	328	323	336
5.8-m WD[c]	291	309	297	339	NA	331	NA	356	340	343	NA	NA	313	312	322	322	155	133	150	133	NA	NA	NA	NA
11.1-m WD	292	301	299	309	321	336	344	4	349	350	346	NA	NA	338	NA	338	158	162	NA	151	NA	333	NA	342
18.9-m WD	300	307	309	318	324	331	351	359	344	351	343	NA	348	350	346	350	158	164	152	150	333	327	338	333
4.1-m Perp[e]	0.8	NA	0.9	NA	1.0	1.0	1.0	1.0	4.3	5.1	4.2	NA	1.1	0.9	1.3	0.9	–1.9	–1.6	–1.5	–1.4	1.5	1.8	1.3	1.6
5.8-m Perp[c]	0.9	1.3	1.1	1.7	NA	1.1	NA	1.1	5.0	5.8	NA	NA	1.1	1.0	1.3	1.4	–2.0	–1.5	–1.8	–1.4	NA	NA	NA	NA
11.1-m Perp	1.0	1.5	1.2	1.7	1.0	1.3	1.1	1.2	5.6	6.2	5.2	NA	NA	1.9	NA	2.0	–2.4	–2.4	NA	–2.1	NA	2.0	NA	1.7
18.9-m Perp	1.8	2.4	2.4	3.0	1.7	1.8	1.8	1.9	8.3	8.9	7.6	NA	2.9	3.0	3.4	3.6	–4.0	–4.0	–3.1	–3.1	2.5	2.3	2.0	2.0
10.1-m Temperature[f]	10.2	9.4	10.6	10.3	12.7	12.6	12.6	12.5	9.8	9.9	9.9	NA	9.2	9.1	7.3	7.3	1.3	1.9	4.1	3.6	2.7	2.8	2.9	3.0
Heat Flux 0–30 min[g]	–17	NA	9	–38	NA	–1	NA	–1	–32	–55	1	–48	7	–1	21	–21	–14	–7	–13	–35	NA	NA	NA	NA
Heat Flux 30–60 min	6	–23	32	–21	NA	–1	NA	1	–24	–63	NA	NA	11	–12	1	–15	–17	7	–7	–29	NA	NA	NA	NA
Background CO	0.150		0.175		0.575		0.717		0.175		0.250		0.110		0.108		0.250		0.200		0.200		0.350	
Downwind CO 3.2 m[h]	0.500		0.458		0.375		0.350		0.138		0.167		0.430		0.392		0.525		0.600		0.183		0.300	
Downwind CO 9.8 m	0.392		0.242		0.225		0.193		0.038		0.017		0.200		0.158		0.217		0.200		0.083		0.117	
Downwind CO 18 m[i]	0.117		0.058		0.075		–0.025		–0.063		–0.033		0.050		0.042		0.033		0.033		0.000		–0.017	
Eastbound Traffic[j]	2714		5583		2491		4934		2620		4684		4466		3040		2587		2496[k]		2069		3892	
Westbound Traffic	2893		4186		3349		4323		3273		4197		4120		3374		3484		3266[k]		3331		4092	

[a]Predominant wind was from the south for these time periods; [b]Wind speed (WS) in m/sec; [c]South 5.8-m sonic is 40.2 m closer to I-80 than the 18-m tower instruments are; [d]Normalized wind direction (WD) orientation (see Figure 1); [e]Perpendicular wind speed (Perp) in m/sec (positive indicates wind from the north); [f]Temperature in °C; [g]Watts/m^2; [h]Downwind concentrations presented with the background removed (ppmv); [i]Negative concentrations occur when background CO exceeds downwind CO; [j]VPH; [k]Loop counters unavailable (traffic estimated from historical data and video counts).

In calculations where a 1-hr averaged CO concentration was subtracted from a 1-hr averaged background concentration, the standard deviation of the difference can be shown to be 0.058 ppmv. Since the random error of each 5-min CO measurement will in part cancel out, the signal-to-noise ratio for a 1-hr average is far superior to that of the 5-min averages and can be used with greater confidence. Inspection of Table 3 indicates that four CO concentrations are reported as negative (–0.017, –0.025, –0.033, and –0.063 ppmv). All four of these measurements occurred at the downwind 18-m sampling port where the CO concentration approached the background at times. These negative concentrations are obviously nonphysical and result from sampling error, but the spread of these values is consistent with the analytical determination of the 1-hr averaged CO concentration's random error.

Meteorological Conditions during Each Sampling Day

The UCD CO sampling began November 14, 1996. At approximately 5:00 a.m., the 0.6-m temperature was ~4 °C colder than the 18-m temperature, indicating a temperature increase of ~1 °C/5 m. The 10-m wind speed was ~2.7 m/sec with a 6° standard deviation of the horizontal wind direction. The heat flux determined by the upwind sonic anemometer varied from –38 to –21 W/m^2. Thus, the stability class during this time period was stable to extremely stable (class E–G depending on the stability criteria applied). The combined traffic flow rate during the November study approached 10,000 vehicles per hour (VPH). The meteorological conditions during the November 21, 1996, study were similar to the first sampling day, but the temperature inversion was significantly less intense.

The wind speed during the November 26, 1996, sampling period was exceedingly high. The ground-level wind speed was typically greater than 5 m/sec, and the wind speed at 18 m exceeded 10 m/sec at times. Given the strong winds, the balloon and tethersonde stations were not used, and only the fixed tower stations collected CO data. Although the wind speeds were strong, the wind directions were approximately constant, with a 1-hr averaged standard deviation of less than 3° at the upwind station.

The December 1, 1996, sampling was the only nighttime sampling for this study and was selected because an evening rush hour was expected due to the Thanksgiving holiday weekend. The CALTRANS hourly counts indicate that the hourly traffic flow rate approached 8500 VPH during the sampling period (6:00–8:00 p.m.) and was comparable in magnitude to the morning commute-hour studies. The ground-level wind speed during the sampling period varied between 1 and 2 m/sec. It is worth noting that for a brief period, the ground-level wind speed at the north tower approached a near-parallel wind speed of 0.8 m/sec. If these low, parallel wind conditions had persisted, it would have been possible to conduct a buoyancy analysis of the type originally envisioned.

The wind was from the south during the December 3, 1996, and January 8, 1997, sampling periods. Since the experiment was designed for a northerly wind, the experiment was not conducted for the full 2 hours on these days. In addition, CALTRANS traffic counts were not available for the January 8, 1997, sampling, making a complete analysis difficult. The last study was conducted January 10, 1997. Wind speeds during this period were also well above 1 m/sec and were qualitatively similar to the first two sampling periods.

EMISSION FACTOR ANALYSIS

Three separate methods were used to determine the CO EF for the I-80 vehicle fleet. The first method was based on the CT-EMFAC (release 2.01) model, the second method was based on back-calculating the CO EF from experimental measurements, and the last method was based on computing the best fit between the observed data and CALINE4-predicted CO concentrations.

CT-EMFAC CO Emission Factor

The California Air Resources Board (ARB) has developed, and currently supports, a modeling tool known as EMFAC to estimate vehicular emission factors for various pollutants. The model is similar to the U.S. Environmental Protection Agency model MOBILE, but it takes into account the vehicle fleet, fuel, and maintenance programs specific to California. The model CT-EMFAC was developed by CALTRANS to simplify estimation of composite EFs based on user-supplied estimates of vehicle fleet operating modes (i.e., cold-start percentage) and vehicle mix distributions (i.e., percentage of heavy-duty trucks). CT-EMFAC is essentially a front-end to the EMFAC model that enables microscale modelers to run analyses without mastering the entire EMFAC model. Thus, CT-EMFAC results can be generalized to the EMFAC model as well.

Transportation planners can estimate CT-EMFAC input parameters based on the California Carbon Monoxide Protocol[11] (CCMP) recommendations and experience. In this study, a variety of input parameters are used to demonstrate the sensitivity of the CT-EMFAC model to user input. The CCMP recommendation for a California vehicle fleet distribution is presented in Table 4. Table 5 lists the hot-stabilized CO EF for various vehicle classes based on a 1996 distribution of vehicle age. Table 5 indicates that the LDA, LDT, and MDT CO EFs are essentially identical at high speeds (see Table 4 for acronym definitions). Heavy-duty gas trucks have significantly higher CO EFs than LDAs at all speeds, whereas HDD CO EFs are

Table 4. Vehicle distribution assumed for the calculation of CO emission factors.

Vehicle Type	Percent of Fleet
Light-duty automobiles (LDA)	69
Light-duty trucks (LDT)	19.4
Medium-duty trucks (MDT)	6.4
Heavy-duty gas trucks (HDG)	1.2
Heavy-duty diesel trucks (HDD)	3.6
Motorcycles (MC)	0.4

Table 5. Hot-stabilized CO EF (g/vehicle-mile) for various vehicle classes operating at 40 °F.

Speed (mph)	LDA	LDT	MDT	HDG	HDD	MC
50	3.2	3.2	3.4	18.5	6.7	5.9
55	3.6	3.8	3.8	20.2	7.0	5.7
60	5.9	6.1	6.3	23.3	7.6	5.2
65	13.4	14.9	15.6	28.4	8.6	3.7

comparable at high speeds. Thus, the CO EF is relatively insensitive to vehicle distribution unless the heavy-duty gas vehicle fraction exceeds 10%, which did not occur during the sampling effort. Therefore, it is unlikely that a slight misestimation of the I-80 vehicle fleet distribution will have a significant impact on the estimated CO EF.

In addition to the vehicle distribution, CT-EMFAC requires the user to estimate the percentage of the vehicle fleet operating in cold, hot, and stabilized running modes. The CCMP recommends that hot spot modelers select a cold-start percentage ranging from 1 to 15 for the observed roadway. The range of possible cold-start percentages results from differing assumptions about the freeway classification, with the lower percentages representing segments with fewer expected modal changes. The lack of any significant on-ramps within 3–5 mi of the experimental site suggests a lower cold-start fraction, 0–5%, for the vehicle fleet was appropriate.

Figure 5 presents the modeled CT-EMFAC CO EFs for various vehicle fleet and operation mode distributions for an ambient temperature of 40 °F (a typical ground-level temperature recorded during the sampling effort). The 100% LDA fleet operating in stable mode (square markers) represents the lowest CO EF value one could reasonably expect for the observed roadway. The CCMP vehicle fleet with 5% cold start is a vehicle distribution that a transportation engineer would presumably select as a default value. Clearly the differences between the baseline and CCMP distributions are relatively insignificant at high speeds. Only if one considers an unreasonably high cold start of 50% (Figure 5, diamond marker) does one see a significant impact in CO EFs.

The approximate average vehicle speed during the study was calculated from video counts to be at least 70 mph; however, CT-EMFAC is only capable of estimating CO emission factors for an average speed of 65 mph or less. Inspection of Figure 5 demonstrates that the CO EF sharply increases when the average vehicle speed is in excess of 55 mph, but it is unclear if this trend continues at higher speeds. To estimate CO EF at speeds greater than 65 mph, a quadratic extrapolation was assumed for the 55–65 mph CT-EMFAC EF values. This reasoning is consistent with the argument that the engine load is proportional to the square of the vehicle speed in this speed range. In reality, residence time on the catalyst bed may be a more realistic explanation for increased emissions, which would suggest that the EF should be linearly extrapolated.

The 65-mph EF for a 5% cold-start fleet is ~15 grams per vehicle mile traveled (GPVMT). One would obviously expect that the 70-mph EF would be greater than the 65-mph EF; thus, 15 GPVMT represents the lowest EF that a traffic engineer could reasonably select using known or predicted values. If a traffic engineer assumed that the CT-EMFAC curve increased linearly, the calculated EF for 70 mph would be ~22 GPVMT; parabolically, it would be 28 GPVMT.

CO Emission Factor Estimation from Field Measurements

It is also possible to directly calculate a composite vehicle fleet CO EF from the field data collected in this study. The relationship between line source strength, vehicular flow rate, and EF is

$$SS = EF \times Q \tag{4}$$

where SS is CO source strength of roadway (g CO per mph); EF is vehicular emission factor (g CO per vehicle per mi); and Q is vehicular flow rate (VPH). Given Q, one can compute an EF if a method for determining SS is available. One way of determining SS from the field data collected in this study is to perform a numerical integration of the CO flux based on curve-fitting of the CO and wind profiles as shown in eq 5.

$$SS = \int_{z_0}^{L} U_{\perp}(z)\, CO(z)\, \kappa \, dz \tag{5}$$

where $U_{\perp}$ is average perpendicular wind speed (m/sec); CO is average CO concentration (g/m^3); z is elevation (m); κ is unit correction factor; L is upper boundary considered in the flux calculations (m); and z_0 is roughness length (m).

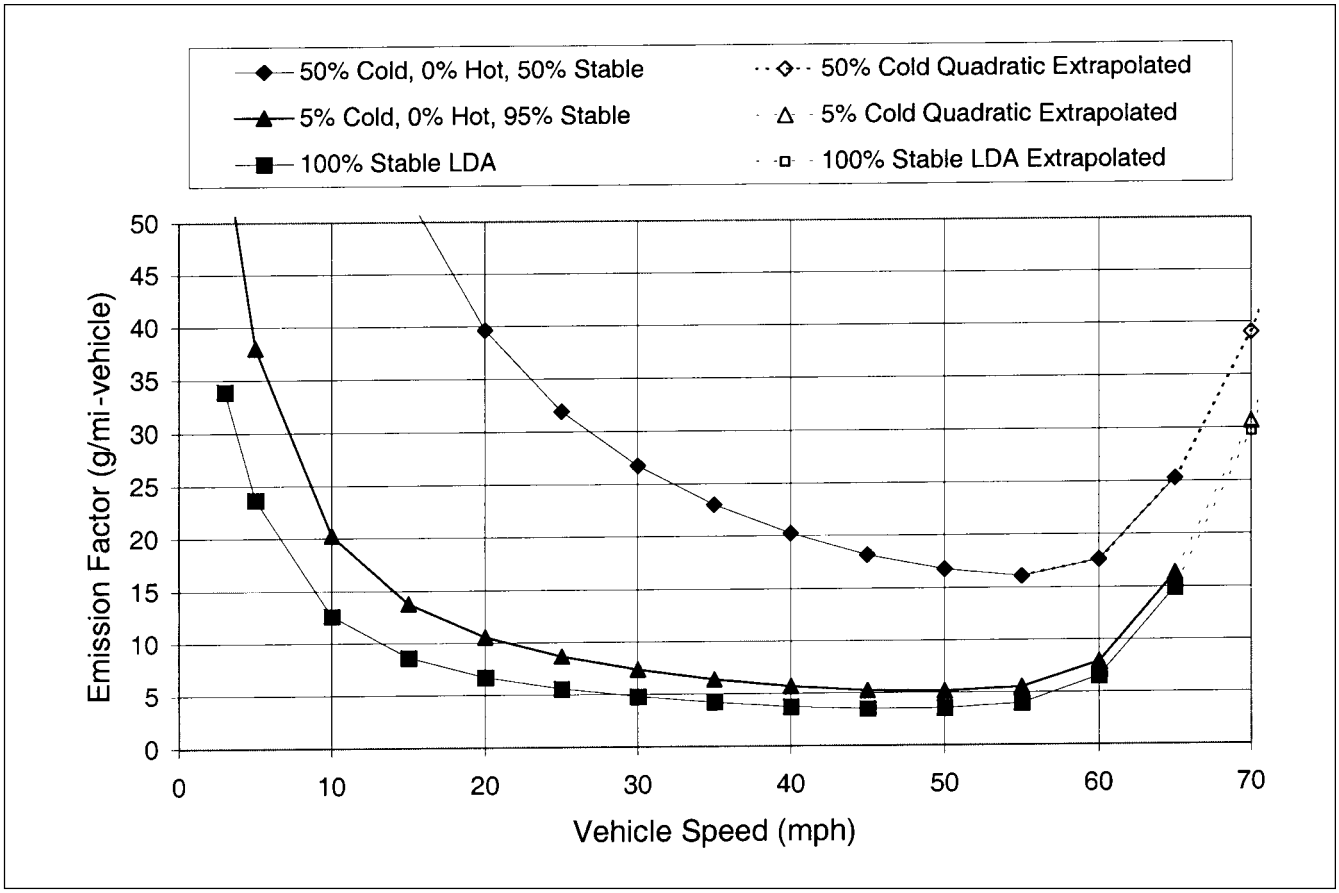

Figure 5. CT-EMFAC emission factors for various fleet compositions. Diamond and triangle series based on vehicle distribution presented in Table 4.

Given that the topography near the highway (due to oleanders in the highway median) is complex and the freeway traffic is a significant source of turbulence, it is unclear whether the log-wind profile or a diabatic wind profile is more representative downwind of the roadway. In this study, it was assumed that the wind speed was adequately described by a neutral logarithmic wind profile that did not have significant wind direction rotation with height for the first few tens of meters above the ground (see eq 6). The friction velocity and surface roughness were determined using a Marquardt least-squares nonlinear fitting for each 1-hr time period. These assumptions should be satisfactory for a first-order approximation of SS.

$$U_{\perp} = \frac{u_{*\perp}}{k} \ln \frac{z}{z_0} \qquad (6)$$

where $u_{*\perp}$ is friction velocity based on perpendicular wind (m/sec), and k is the von Karman constant (0.4).

The exact functional form of the CO profile is also unknown. For a first-order approximation, it was assumed that the CO profile decreased exponentially with height. This functional form does not have a rigorous theoretical basis; however, it exhibited good agreement with the 1-hr CO samples with the background removed. A linear function also fit the data set quite well and was used for comparison purposes. Once the functional forms of U and CO were determined, the effective source strength of the road was calculated by eq 5 and the EF was back-calculated from eq 4.

The method derived above is based on the following assumptions:

- The CO and wind fields are steady over the averaging time of the CO bag sample;
- The functional forms selected to represent the CO and wind profiles are valid;
- The CO profile results from an upwind infinite line source (i.e., there are no edge effects at the end of the line source);
- There is no pollutant flux above the top control element considered;
- There is negligible pollutant flux between 0 m and z_0;
- The emission source strength is linearly proportional to vehicle count; and
- The along-wind diffusive flux is insignificant in comparison with the advective flux.

Given the meteorological and traffic conditions experienced in the field, these assumptions appear to be valid. The most questionable assumptions made in this

analysis were the functional forms selected for the CO and wind profiles. However, we feel that the assumed CO and wind profiles were sufficiently accurate for a first-order estimate. It should also be noted that the CO concentration profile typically approached 0 ppmv prior to the upper elevation CO port. Thus, it is unlikely that there was a significant flux of CO overlooked when the definite integral upper bound for eq 5 was considered finite. For the linearly-fit CO profile calculations that follow, L was varied from 16 to 23 m to ensure that the CO flux at upper elevations could not be negative (upper-elevation negative fluxes are expected given a linear functional form of the CO profile). For the exponential fit, L was considered to be 4 times the L from the linear fit (~60 m) to ensure that at least 99% of the CO flux was considered in the flux integral.

A program was written to numerically back-calculate a composite EF based on 1-hr averaged wind and CO profiles for each period that CALTRANS hourly traffic counts, wind speed, wind direction, and CO measurements were available. Results of the analysis are shown in Table 6. The average EF for the twelve 1-hr periods considered was calculated to be 6.4 GPVMT with a standard deviation of 2.8 for the linear CO fit, and 6.8 GPVMT with a standard deviation of 3.3 for the exponential CO fit. Insufficient data were available to determine why the CO EF for the two periods of southerly wind were significantly greater than the EF for the ten periods of northerly wind. Figure 6 shows the wind, CO, and CO flux profiles for two periods for both the linear and exponential fit CO profiles. The shape of the flux profile is as expected and demonstrates that an insignificant amount of mass is lost above elevation L or below z_o.

Table 6. CO emission factor (GPVMT) back-calculated from downwind CO and wind profiles.

Time Period	Linear CO Profile	Exponential CO Profile
Nov 14, 6:00–7:00 a.m.	8.9	13.0
Nov 14, 7:00–8:00 a.m.	4.7	5.4
Nov 21, 6:00–7:00 a.m.	5.7	7.3
Nov 21, 7:00–8:00 a.m.	2.8	3.2
Nov 26, 6:00–7:00 a.m.	7.1	6.5
Nov 26, 7:00–8:00 a.m.	4.7	3.5
Dec 1, 6:00–7:00 p.m.	5.9	6.6
Dec 1, 7:00–8:00 p.m.	8.0	8.3
Dec 3, 6:00–7:00 a.m.	10.7	11.1
Jan 8, 6:00–7:00 a.m.	11.1	10.1
Jan 10, 6:00–7:00 a.m.	3.6	3.8
Jan 10, 7:00–8:00 a.m.	3.2	3.3
Average	6.4	6.8
Standard Deviation	2.8	3.3

CALINE4 Analysis

By minimizing the total squared residual between the measured and CALINE4-predicted CO concentrations at the downwind 18-m and 6-m towers for the eleven 1-hr periods with complete data, a CO EF for the vehicle fleet traveling on I-80 could be computed. The CO EF calculated from this method was 6.5 GPVMT. For human health concerns, only the lower-elevation CO predictions are of interest. When only CO concentrations at elevations less than 6 m were considered, the EF with the minimized sum of squares residual was found to be 7.0 GPVMT.

The CALINE4 simulations were based on the collected field data (i.e., field-measured σ_θ was used rather than default settings). Although CALINE4 is a relatively simple model to run, the wind-speed input is worth clarifying. According to the user manual, the wind speed should be "measure[d] at 5 to 10 m or assume worst-case. For localized sources and nearby receptors, wind speeds measured at lower elevations (5 m) [are] desirable…."[1] In this analysis, the wind speed used was from the upwind 4-m wind sensor. Noting that CO concentrations are inversely proportional to wind speed, a wind speed measured at a higher elevation will result in a lower downwind CO concentration since wind speed typically increases with height. Futhermore, if CO concentrations are held constant, an increase in wind speed would require an increase in EF.

Figures 7 and 8 present the measured and CALINE4-modeled CO concentrations based on two different emission factors for the November 21, 1996, 6:00 to 7:00 a.m., and December 1, 1996, 6:00 to 7:00 p.m., sampling periods. The 7.0 GPVMT line represents the minimized sum of squares residual fit EF, and 22 GPVMT is considered the EF that a traffic engineer would select based on the CT-EMFAC analysis. Clearly an EF of 7.0 GPVMT matches the measured CO concentrations more accurately than 22 GPVMT does. For instance, in Figure 8 the measured and predicted CO concentrations at the lower freeway tower sampling port for an EF of 7.0 are nearly identical, whereas the EF of 22 results in an overprediction of ~340%. The remaining 1-hr time periods also demonstrate the trends presented in Figures 7 and 8 for the balloon and tower stations. Thus, CALINE4 appears to provide reasonable estimates of dispersion 30–60 m from a roadway if accurate emissions input data are supplied during non-worst-case meteorological conditions.

Since 7.0 GVPM is the best-fit EF, there are several instances where CALINE4 underpredicted CO concentrations near the observed highway. Thus, it would appear warranted to multiply the best-fit EF by a safety factor (SF) so that CO concentration estimates would be conservative. However, applying an SF greater than

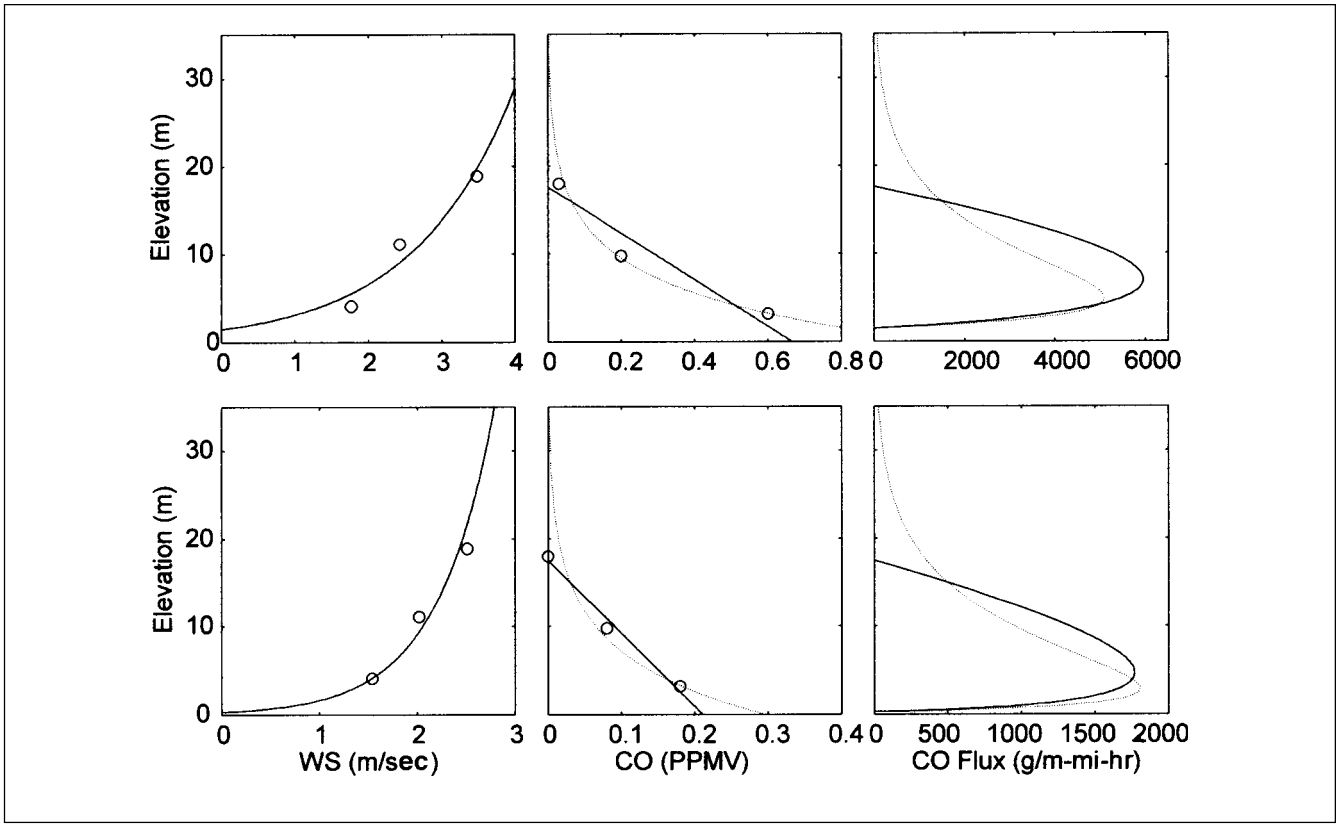

Figure 6. Wind speed, CO concentration, and CO flux profiles downwind of I-80. Dashed lines are exponentially fit and solid lines are linearly fit for the CO and CO flux subplots. The top three plots are for the January 8, 6:00–7:00 a.m. sampling period when the wind was from the south. The bottom three plots are for the January 10, 6:00–7:00 a.m. sampling period when the wind was from the north.

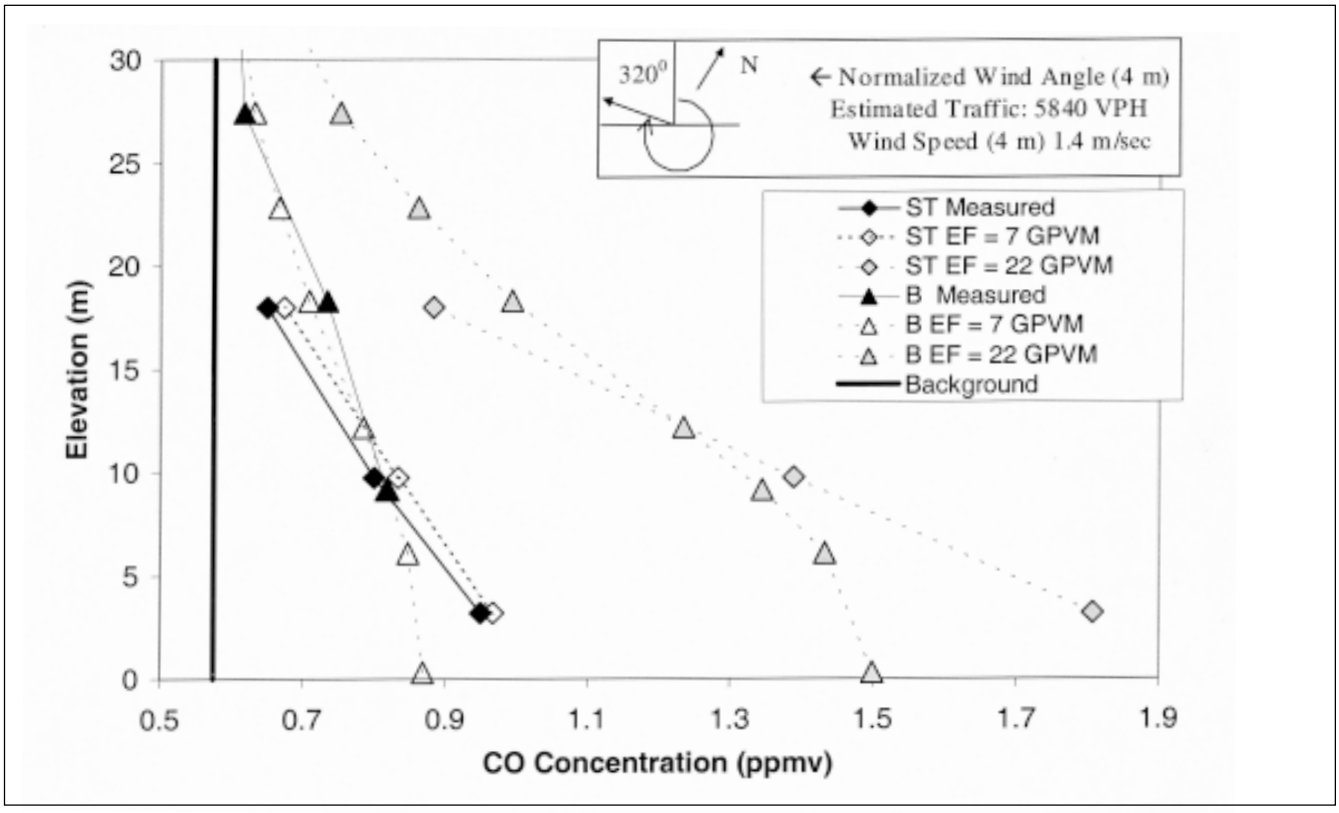

Figure 7. Measured and CALINE4-predicted CO concentrations for the November 21, 1996, 6:00–7:00 a.m. sampling period for two different CO emission factors. Wind angle orientation based on standard meteorological convention. ST = south tower; B = balloon station.

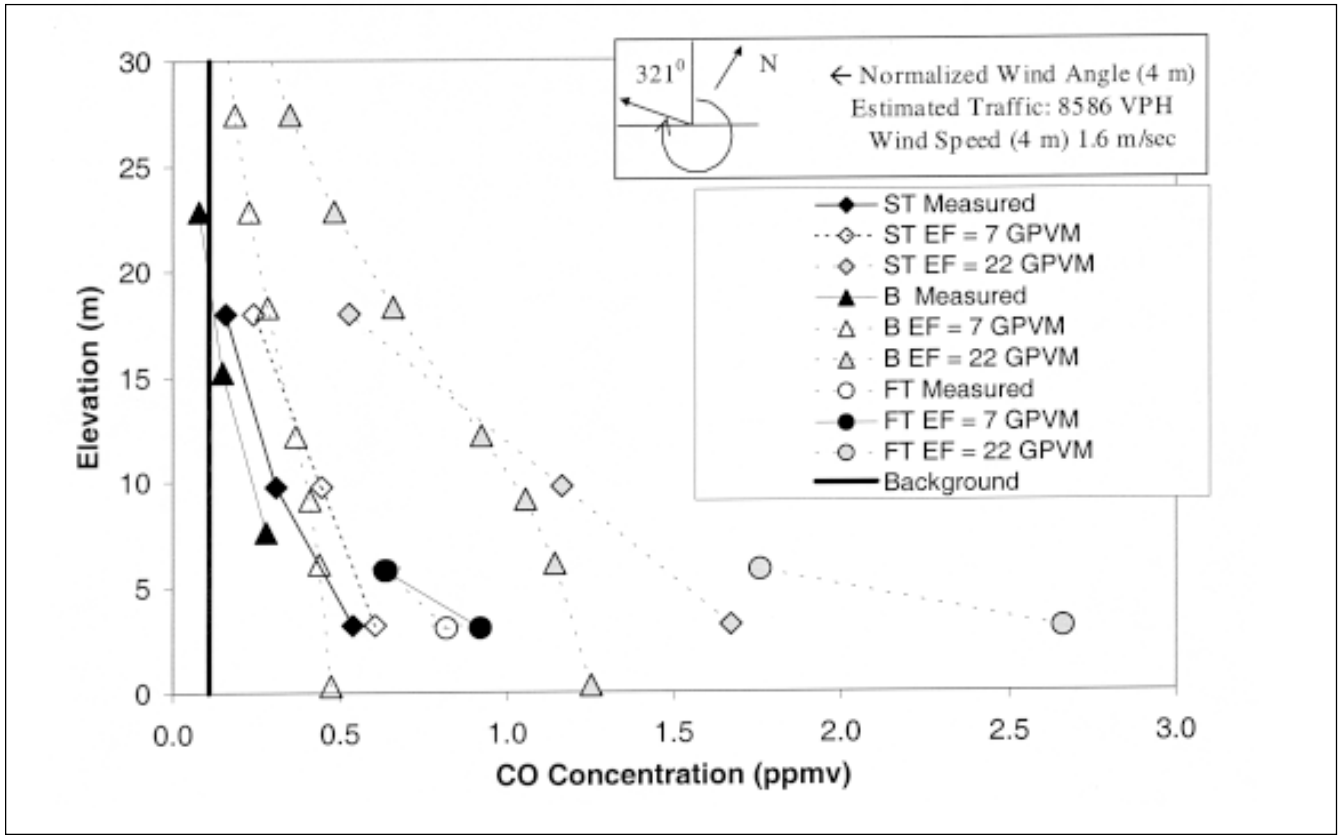

Figure 8. Measured and CALINE4-predicted CO concentrations for the December 1, 1996, 6:00–7:00 p.m. sampling period for two different CO emission factors. Wind angle orientation based on standard meteorological convention. ST = south tower; B = balloon station; FT = freeway tower.

3 would result in a CO EF similar to the one predicted by CT-EMFAC. This appears to obviate the need for the additional EF analysis performed in this study, since we are suggesting the use of an EF similar to the CT-EMFAC model. In reality, this is not an "apples to apples" comparison, because the CT-EMFAC model is intended to produce exact, not conservative, EFs. As it stands, the transportation planner has no practical intuition whether an EF from CT-EMFAC or CALINE4 already has a built-in SF, or whether one needs to be used. Efforts should be made to provide transportation/air-quality modelers with guidelines indicating where and when SFs should be used for screening purposes and to clearly state what implicit and explicit SFs are present in both emission factor and dispersion models.

The downwind concentrations observed near the roadway are quite low, typically ranging from 0 to 1 ppmv, and are in no danger of violating the California or federal CO standard. Observed CO concentrations in this study were low due to the modest traffic loading and near-zero background concentration. In areas where the background CO concentration is greater, the roadway contribution necessary to exceed the air quality standard would be less. Thus, the overestimation of the CO EF would probably be most significant near freeways with greater traffic loading in an area with an ambient background CO concentration approaching the regulatory standard.

CONCLUSIONS

Three methods were used to determine the CO EF for a vehicle fleet traveling on a freeway near Davis. CT-EMFAC, which would presumably be used by a traffic engineer to perform a screening analysis of a proposed or existing roadway, resulted in a CO EF prediction of approximately 15–28 GPVMT. A CO EF back-calculated from the integrated highway CO flux was found to be ~6.4 or 6.8 GPVMT. Lastly, CALINE4 was used to minimize the error between measured and modeled CO concentrations and resulted in a CO EF of ~7 GPVMT. Figures 7 and 8 are representative of the twelve 1-hr sampling periods and demonstrate that an EF of 7.0 GPVMT provides excellent agreement between measured and CALINE4-predicted concentrations. It appears that a CO EF of 7 GPVMT is much more appropriate for the observed roadway than the 15–28 GPVMT that would be predicted by the CT-EMFAC model. Futhermore, since a predicted downwind CO concentration is linearly proportional to the CO EF, a 100% error in EF estimation will lead to a 100% error in predicted CO concentrations.

There are some limitations associated with the techniques employed in this study. Specifically, the downwind CO and wind profiles were limited to three points for each 1-hr average. Although the three-point curves appear to adequately fit the CO profile, the log wind profile and the measured wind profile did not show strong agreement for every 1-hr time period. While the functional form of the CO and wind profiles may not be exact, the methodology for calculating the CO flux is still suitably robust to demonstrate the significant difference between measured and modeled CO EF.

The EMFAC model was originally designed for *regional* air quality modeling of mobile emissions. The CT-EMFAC model uses selected features of the EMFAC model to estimate an *aggregate* EF for a vehicle fleet traveling at a *trip-averaged speed*. However, for "hot-spot" analysis, a *modal* EF representing vehicle fleet emissions by *mode of operation* (i.e., traveling at 25 mph or idling) is required. Thus, improperly using regional emission factors to determine modal emissions introduces significant error into microscale analysis and highlights the need for new modal emission factor models designed expressly to perform facility-specific microscale air quality studies.

ACKNOWLEDGMENTS

Support for this study was provided by CALTRANS under the guidance and direction of Steve Borroum. Additional assistance from CALTRANS was provided by Keith Jones, Doug Eisinger, Marianne Larsen, and Tom Kear. The authors gratefully acknowledge Dr. Roger Shaw, Dr. Kyaw Tha Paw U, Dr. John Carroll, and Ed Tai for their support and insight. Lastly, the authors would like to thank the crew members, whose hard work made these experiments possible: George Croll, Kellie Dougherty, Dale Uyeminami, Sid Sok, Vicente Garza, and Pingkuan Di.

REFERENCES

1. Benson, P.E. *CALINE4, a Dispersion Model for Predicting Air Pollutant Concentrations Near Roadways*; California Department of Transportation: 1984.
2. Nanzetta, K.; Niemeier, D.; Utts, J.M. Changing Speed-VMT Distributions: The Effects on Emissions Inventories and Conformity; *J. Air & Waste Manage. Assoc.* **2000**, *50*, 459-467.
3. California Air Resources Board. *Methodology for Estimating Emissions from On-Road Motor Vehicles;* Volume I–III, 7f; Prepared by Technical Support Division Mobile Source Emission Inventory Branch, California Air Resources Board: September 1993.
4. California Air Resources Board. *Methodology for Estimating Emissions from On-Road Motor Vehicles*; Volume I–VII, 7g; Prepared by Technical Support Division Mobile Source Emission Inventory Branch, California Air Resources Board: December 1995.
5. National Research Council. *Modeling Mobile-Source Emissions*; Washington, DC, Committee To Review EPA's Mobile Source Emissions Factor Model; Board on Environmental Studies and Toxicology; Commission on Geosciences, Environment, and Resources; Transportation Research Board; National Research Council: 2000.
6. Moseholm, L.; Silva, J.; Larson, T. Forecasting Carbon Monoxide Concentrations near a Sheltered Intersection Using Video Traffic Surveillance and Neural Networks; *Transportation Research Part D: Transport Environment* **1996**, 1D.
7. Scully, R.D. Vehicle Emission Rate Analysis for Carbon Monoxide Hot Spot Modeling; *J. Air Pollut. Control Assoc.* **1989**, *39*, 1334-1343.
8. Zamurs, J.; Conway, R. Comparison of Intersection Air Quality Model's Ability to Simulate Carbon Monoxide Concentrations in an Urban Area; *Transport. Res. Record* **1991**, 23-32.
9. Held, A.E.; Chang, D.P.Y.; Carroll, J.J. *Observations and Model Simulations of Carbon Monoxide Dispersion*; California Department of Transportation: 1998.
10. Wilson, J.D.; Swaters, G.E. The Source Area Influencing a Measurement in the Planetary Boundary Layer—The Footprint and the Distribution of Contact Distance; *Boundary-Layer Meteorol.* **1991**, *55*, 25-46.
11. Garza, V.J.; Franey, P.; Sperling, D. *Transportation Project-Level Carbon Monoxide Protocol*; Institute of Transportation Studies, University of California, Davis: Davis, CA, 1996.

About the Authors

Anthony Held is currently a doctoral student at the University of California, Davis. The work presented in this paper was the foundation of his Master of Science research. Please address all correspondence to Anthony Held, Department of Civil and Environmental Engineering, One Shields Ave., Davis, CA 95817; e-mail: aeheld@ucdavis.edu. Daniel P.Y. Chang is a professor of Civil and Environmental Engineering and currently serves as chair of the department. His research interests are in the areas of physico-chemical and biological air pollution control, by-products of combustion processes, dispersion modeling, and health effects. Debbie Niemeier is an associate professor in the Department of Civil and Environmental Engineering. Her research interests are in the areas of transportation forecasting and modeling of mobile emissions.